methyl-3-pentanone, 565-80-0; 2-methyl-3-isopropyl-6-hepten-3-ol, 38443-89-9; 2,3-dimethyl-3-butene, 563-78-0; 2,3-dimethyl-2-butene, 563-79-1; 2,5,6-trimethyl-3-isopropyl-6-hepten-3-ol-*4,4,7,7-d*$_4$, 115982-94-0; 2,5,6-trimethyl-3-isopropyl-6-hepten-3-ol, 115982-95-1; 2,4,5-trimethyl-5-hexen-2-ol-*3,3,6,6-d*$_4$, 115982-96-2; 2,4,5-trimethyl-5-hexen-2-ol, 115982-97-3; acetone, 67-64-1.

Supplementary Material Available: Listings of atomic coordinates for hydrogen atoms with isotropic temperature factors, anisotropic thermal parameters for non-hydrogen atoms, and bond distances and angles including hydrogen atoms (3 pages); a listing of observed and calculated structure factors (48 pages). Ordering information is given on any current masthead page.

Preparation and Structure of $Ru_3(CO)_7(\mu_3\text{-}\eta^2\text{-}C_6H_4)(\mu\text{-}PPhFc)_2$

William R. Cullen* and Stephanie T. Chacon

Department of Chemistry, University of British Columbia, Vancouver, British Columbia, Canada V6T 1Y6

Michael I. Bruce

Department of Physical and Inorganic Chemistry, University of Adelaide, Adelaide, South Australia

Frederick W. B. Einstein* and Richard H. Jones

Department of Chemistry, Simon Fraser University, Burnaby, British Columbia, Canada V5A 1S6

Received November 20, 1987

Heating $Ru_3(CO)_{10}(PFcPh_2)_2$, FcH = $Fe(\eta^5\text{-}C_5H_5)_2$, in refluxing cyclohexane affords a good yield, 83%, of the μ_3-benzyne complex $Ru_3(CO)_7(\mu_3\text{-}\eta^2\text{-}C_6H_4)(\mu_2\text{-}PPhFc)_2$ (**2e**), which was characterized by X-ray diffraction. It crystallizes in the monoclinic system, space group $P2_1/n$, with cell constants a = 17.872 (2) Å, b = 13.017 (1) Å, c = 18.547 (2) Å, and β = 101.50 (1)°; the final R value of 0.028 was obtained by using 3526 observed reflections. The Fc groups are trans with respect to the plane of the Ru_3 triangle. The benzyne fragment, which seems to have partially localized bonds, is planar and makes an angle of 64.0 (2)° with the plane of the Ru_3 triangle. NMR studies of the fluxional behavior of the benzyne fragment, a 180° rotation, indicate that the motion is less facile than is found in related Os_3 systems.

Introduction

Dehydrobenzene, benzyne, is a highly reactive molecule[1] which can be trapped as simple η^2-bound metal complexes such as 1 (M = Ta)[2] and μ_3-η^2-bound complexes such as **2a**.[3,4a] Some examples of μ_4-η^2-binding are known, e.g. **3**.[4]

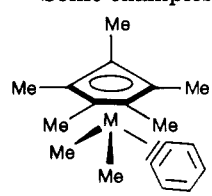

1

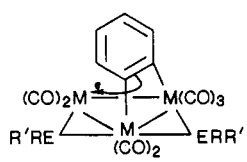

2a-f

a, M = Os, ERR′ = PPh_2; **b**, M = Ru, ERR′ = PPh_2; **c**, M = Os, ERR′ = PMe_2; **d**, M = Os, ERR′ = $AsMe_2$; **e**, M = Ru, ERR′ = PFcPh; **f**, M = Ru, ERR′ = PFcPh, PPh_2

There are few reports concerning the possibility that dehydroferrocene, ferrocyne, has an independent existence.[5] One of the objectives of our current research efforts is to establish if ferrocyne can be trapped as a metal complex by using similar techniques to those used for the preparation of **1**–**3**. Hope in this endeavor is fueled by work showing that complexes such as **4** are stable.[6]

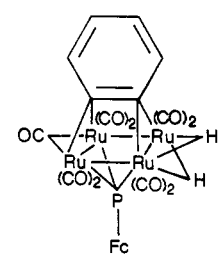

3

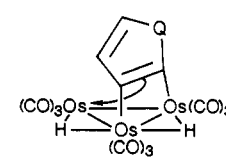

4

Furthermore, the dehydrocyclopentadienyl ion seems to be capable of transient existence.[7] This paper describes an attempt to trap ferrocyne by pyrolysis of the complex $Ru_3(CO)_{10}(PFcPh_2)_2$,[8] FcH = $Fe(\eta^5\text{-}C_5H_5)_2$. It seems that P–Ph bond cleavage is more facile than P–Fc so that the principal product is **2e**. The crystal structure of this new compound is described as are NMR studies of the fluxional

(1) (a) Huisgen, R. In *Organometallic Chemistry*; Zeiss, H., Ed.; Reinhold: New York, 1960; Chapter 2. (b) Fieser, L. F. *Organic Chemistry*; Reinhold: New York, 1961. (c) Gilchrist, T. L.; Rees, C. W. *Carbenes, Nitrenes, and Arynes*; Nelson and Sons: London, 1969.

(2) (a) Bennett, M. A.; Hambley, T. W.; Roberts, N. K.; Robertson, G. B. *Organometallics* **1985**, *4*, 1992. (b) McLain, S. J.; Schrock, R. R.; Sharp, P. R.; Churchill, M. R.; Youngs, W. J. *J. Am. Chem. Soc.* **1979**, *101*, 263. (c) Churchill, M. R.; Youngs, W. J. *Inorg. Chem.* **1979**, *18*, 1697. (d) Buchwald, S. L.; Watson, B. T. *J. Am. Chem. Soc.* **1986**, *108*, 7411.

(3) E.g. (a) Gainsford, G. J.; Guss, J. M.; Ireland, P. R.; Mason, R.; Bradford, C. W.; Nyholm, R. S. *J. Organomet. Chem.* **1972**, *40*, C70. (b) Bradford, C. W.; Nyholm, R. S. *J. Chem. Soc., Dalton Trans.* **1973**, 529. (c) Bruce, M. I.; Shaw, G.; Stone, F. G. A. *J. Chem. Soc., Dalton Trans.* **1972**, 2094. (d) Deeming, A. J.; Kimber, R. E.; Underhill, M. *J. Chem. Soc., Dalton Trans.* **1973**, 2589. (e) Deeming, A. J.; Rothwell, I. P.; Hursthouse, M. B.; Backer-Dirks, J. D. J. *J. Chem. Soc., Dalton Trans.* **1981**, 1879. (f) Adams, R. D.; Katshira, D. A.; Yang, L.-W. *Organometallics* **1981**, *1*, 235. (g) Brown, S. C.; Evans, J.; Smart, L. E. *J. Chem. Soc., Chem. Commun.* **1980**, 1021. (h) Deeming, A. J.; Underhill, M. *J. Organomet. Chem.* **1972**, *42*, C60. (i) Azam, K. A.; Yin, C. C.; Deeming, A. J. *J. Chem. Soc., Dalton Trans.* **1978**, 1201. (j) Goudsmit, R. J.; Johnson, B. F. G.; Lewis, J.; Raithby, P. R.; Rosales, M. J. *J. Chem. Soc., Dalton Trans.* **1983**, 2257. (k) Bruce, M. I.; Guss, I. M.; Mason, R.; Skelton, B. W.; White, A. H. *J. Organomet. Chem.* **1983**, *251*, 261. (l) Deeming, A. J.; Kabir, S. E.; Powell, N. I.; Bates, P. A. Hursthouse, M. B. *J. Chem. Soc., Dalton Trans.* **1987**, 1520.

(4) (a) Bruce, M. I.; Shawkataby, O. B.; Tiekink, E. R. T.; Snow, M. R., unpublished results. (b) Knox, S. A. R.; Lloyd, B. R.; Orpen, A. G.; Vinas, J. M.; Weber, M. *J. Chem. Soc., Chem. Commun.*, **1987**, 1498.

(5) (a) Huffman, J. W.; Cope, J. F. *J. Org. Chem.* **1971**, *36*, 4068. (b) Huffman, J. W.; Keith, L. H.; Asbury, R. L. *J. Org. Chem.* **1965**, *30*, 1600.

(6) (a) Deeming, A. J. *J. Organomet. Chem.* **1978**, *150*, 123. (b) Arce, A. J.; De Sanctis, Y.; Deeming, A. J. *J. Chem. Soc., Dalton Trans.*, in press. (c) Yin, C. C.; Deeming, A. J. *J. Chem. Soc., Dalton Trans.* **1982**, 2563. (d) Humphries, A. P.; Knox, S. A. R. *J. Chem. Soc., Dalton Trans.* **1975**, 1710.

(7) Martin, J. C.; Bloch, D. R. *J. Am. Chem. Soc.* **1971**, *93*, 451.

(8) (a) Chacon, S. T.; Cullen, W. R.; Einstein, F. W. B.; Jones, R. H.; Willis, A. C., unpublished results. (b) Butler, I. R.; Cullen, W. R.; Rettig, S. J. *Organometallics* **1987**, *6*, 872.

0276-7333/88/2307-2273$01.50/0

behavior of the benzyne moiety.

Experimental Section

The general experimental procedures and instrumentation used for these studies have been described previously.[8b]

Thermal Decomposition of $Ru_3(CO)_{10}(PFcPh_2)_2$. Preparation of 2e. The $Ru_3(CO)_{10}$ derivative[8a] (100 mg) was stable in refluxing hexanes (1 h) and in refluxing 1:1 hexanes/cyclohexane (1 h). The complex decomposed smoothly in refluxing cyclohexane (30 min). Chromatographic workup on alumina using diethyl ether as eluent afforded a good yield (83%) of a red purple solid, **2e**.

^1H NMR (400 MHz, $CDCl_3$): δ 2.88 (s, 2), 3.69 (s, 1), 3.78 (s, 1), 4.00 (s, 5), 4.01 (s, 1), 4.09 (s, 1), 4.29 (s, 5), 4.41–4.44 (m, 2), 4.55 (s, 1), 6.36–6.40 (m, 1), 6.47–6.51 (m, 1), 6.57–6.61 (m, 1), 6.98–7.00 (m, 1), 7.32–7.30 (m, 1), 7.45–7.55 (m, 7), 7.71–7.74 (m, 1), 7.76–7.82 (m, 2), 7.95–8.00 (m, 2). $^{31}P\{^1H\}$ NMR (109.3 MHz, $CDCl_3$): δ 131.0 (d, J(PP) = 200 Hz), 67.8 (d, J(PP) = 200 Hz). Infrared (FT, C_6H_{12}): ν(CO) 2054 s, 2013 m, 2003 s, 1996 m, 1961 sh, 1956 m, 1951 w, 1943 sh cm^{-1}. Mass spectrum (electron impact, probe temperature 240 °C): m/e 1163, 1106, 1079, 1050, 1023, 994, 967, 888, 821, 810, 783, 766, 746, 734, 703, 655, 600, 577, 503, 489, 478, 446, 429, 415, 401, 386, 370, 355, 262, 186, 149, 121, 77, 56.

Anal. Calcd for $C_{45}H_{32}Fe_2O_7P_2Ru_3$: C, 46.52; H, 2.78. Found: C, 46.63; H, 3.59.

Crystal Structure Determination of 2e. A suitable crystal, grown from diethyl ether/hexane, was mounted in a thin-walled capillary and transferred to an Enraf-Nonius CAD4F diffractometer equipped with graphite-monochromated Mo Kα radiation. The unit cell parameters and an orientation matrix were obtained from the accurate setting angles of 25 reflections ($23° < 2\theta < 35°$). Two standard reflections were measured every 5400 s and showed a variation of ±1.5%; these standards were used to scale the data. The data were corrected for Lorentz, for polarization, and empirically for absorption effects.[9] A total 6844 reflections were collected, of which 3534 were considered to be observed ($I > 2.5\sigma(I)$); however, eight reflections with asymmetric backgrounds were eiminated from the refinement of the structure leaving 3526 reflections which were used in subsequent calculations. Pertinant crystallographic and experimental parameters are given in Table I.

The structure was solved by direct methods[10] and refined by full-matrix least squares. Some of the hydrogen atoms were indicated by difference Fourier syntheses, but all the hydrogen atoms were included in their theoretical positions [d(C–H) = 0.95 Å]. The variables included in the refinement were overall scale and positional and anisotropic thermal parameters to all nonhydrogen atoms. The refinement was considered complete when the ratio of calculated shifts to esd's was less than 0.01.

The final residuals were R = 0.0281 and R_w = 0.0334, and the goodness of fit was 0.953. During the final cycles of refinement the weighting scheme employed was $w = 1/(\sigma(F_o))^2 + 0.0006(F_o)^2)$. An analysis showed systematic variation for $\langle w\Delta^2 \rangle$ as a function of either F_o or $(\sin\theta)/\lambda$. The largest peak in the final difference map had a height of 0.43 (8) e A^{-3} and was situated 1.04 Å from Ru(3). Complex neutral atom scattering factors were taken from ref 11. Computer programs were run on an in-house MICROVAX I.[12] Positional parameters are given in Table II. Selected bond distances and interbond angles are listed in Tables III and IV. A SNOOPI thermal ellipsoid plot[13] is given in Figure 1. Anisotropic thermal parameters, hydrogen atom coordinates, and a listing calculated and observed structure factors are available as supplementary material.

Table I

compd	$Ru_3(CO)_7(C_6H_4)\{P(Ph)(Fc)\}_2$
formula	$Ru_3C_{45}H_{32}O_7Fe_2P_2$
mol wt	1161.60
cryst system	monoclinic
space group	$P2_1/n$
a, Å	17.872 (2)
b, Å	13.017 (1)
c, Å	18.547 (2)
β, deg	101.50 (1)
V, Å^3	4228.36
Z	4
D, g cm^{-3}	1.825
cryst dimens, mm	0.39 × 0.20 × 0.11
temp, K	293
radiatn	Mo Kα, λ = 0.71069 Å
μ(Mo Kα), cm^{-1}	18.22
transmissn factors	0.902–0.999
scan mode	coupled $\omega/2\theta$
scan speed range, deg min^{-1}	0.72–2.75
scan width, deg	0.65 + 0.35 tan θ
θ limits, deg	$0.0 < 2\theta \leq 45.0$
data collected	$h,k,\pm l$
unique reflctns	6844
obsd reflctns ($I \geq 2.5\sigma(I)$)	3526
no. of variables	532
R	0.028
R_w	0.033
goodness of fit	0.953

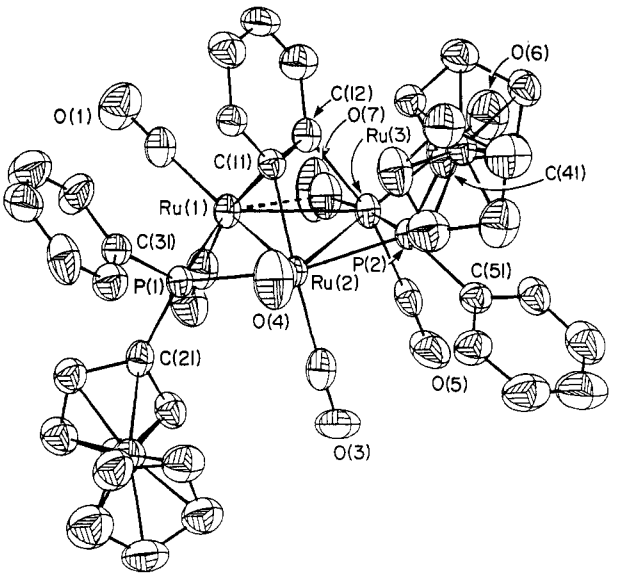

Figure 1. The structure of **2e**. The probability elipsoids are set at the 50% enclosure level.

Results and Discussion

Complexes containing μ_3-η^2-benzyne moieties such as **2** are best prepared by pyrolysis of the simple metal carbonyl derivatives $M_3(CO)_{12-n}L_n$ (M = Ru, Os; n = 1–3; L = PArRR′, AsArRR′).[3] In particular thermolysis of $Os_3(CO)_{10}(PPh_3)_2$ in refluxing xylene affords a number of products resulting from intracluster C–H and C–P bond cleavage and C–C bond formation reactions. Three of these products contain μ_3-η^2-benzyne fragments such as that seen in **2**. One of the three has two bridging phosphido groups **2a**; the other two have one bridging phosphido group and one bridging hydride. The pyrolysis of $Ru_3(CO)_9(PPh_3)_3$ in refluxing Decalin affords **2b** as the only benzyne-containing complex; other dinuclear derivatives are also formed.[3c,k]

The thermal decomposition of $Ru_3(CO)_{10}(PFcPh_2)_2$[8a] takes place under milder conditions in refluxing cyclohexane. Complex **2e** can be obtained in good yield following isolation by chromatography on alumina. Pyrolysis

(9) Alcock, N. W. *Crystallographic Computing*; Ahmed, F., Ed.; Munksgaard; Copenhagen, 1970; p 271.
(10) Germain, G.; Main, P.; Woolfson, M. M. *Acta Crystallogr. Sect. A: Cryst. Phys., Diffr., Theor. Gen. Chem.* **1971**, *A27*, 368.
(11) *International Tables for X-ray Crystallography*; Kynoch: Birmingham, England, 1974; Vol. 4.
(12) (a) Gabe, E. J.; Larson, A. C.; Lee, F. L.; LePage, Y. *NRC VAX Crystal Structure System*; National Research Council of Canada: Ottawa, Ontario, 1984. (b) Watkin, D. J.; Carruthers, J. R.; Betteridge, P. W. *CRYSTALS User Guide*; Chemical Crystallography Laboratory, University of Oxford: Oxford, England, 1985.
(13) Davies, E. K. *SNOOPI Plot Diagram*; Chemical Crystallography Laboratory, University of Oxford: Oxford, England, 1984.

Table II. Atomic Coordinates (Fractional) with Esd's in Parentheses and B_{eq} (Å²) for the Non-Hydrogen Atoms

	x	y	z	B_{eq}
Ru(1)	0.97563 (3)	0.05135 (4)	0.72421 (3)	2.72
Ru(2)	0.97501 (3)	0.24898 (4)	0.78016 (3)	2.34
Ru(3)	1.11221 (3)	0.15433 (4)	0.74975 (3)	2.68
Fe(1)	0.82217 (6)	0.10475 (9)	0.94396 (6)	3.54
Fe(2)	1.05295 (6)	0.55711 (8)	0.65746 (6)	3.31
P(1)	0.88203 (10)	0.12088 (14)	0.77544 (10)	2.63
P(2)	1.08480 (10)	0.33170 (13)	0.76191 (10)	2.49
O(1)	1.0044 (3)	−0.1235 (4)	0.8324 (3)	5.2
O(2)	0.8965 (4)	−0.0875 (5)	0.6024 (4)	6.3
O(3)	1.0251 (3)	0.2615 (5)	0.9490 (3)	5.8
O(4)	0.8665 (4)	0.4279 (5)	0.7594 (4)	7.0
O(5)	1.1935 (3)	0.1551 (5)	0.9112 (3)	5.5
O(6)	1.2427 (3)	0.2137 (5)	0.6748 (3)	6.3
O(7)	1.1462 (3)	−0.0751 (4)	0.7427 (4)	6.6
C(1)	0.9923 (4)	−0.0574 (6)	0.7920 (4)	3.7
C(2)	0.9269 (4)	−0.0363 (6)	0.6498 (5)	3.7
C(3)	1.0055 (4)	0.2568 (6)	0.8881 (5)	3.7
C(4)	0.9081 (4)	0.3591 (6)	0.7679 (4)	3.8
C(5)	1.1659 (4)	0.1535 (6)	0.8511 (4)	3.3
C(6)	1.1950 (4)	0.1889 (6)	0.7026 (5)	4.1
C(7)	1.1238 (4)	0.0055 (7)	0.7417 (5)	4.4
C(11)	0.9607 (4)	0.2137 (5)	0.6665 (4)	2.7
C(12)	1.0275 (4)	0.1660 (5)	0.6520 (4)	2.8
C(13)	1.0298 (5)	0.1374 (6)	0.5776 (4)	3.9
C(14)	0.9704 (5)	0.1587 (7)	0.5223 (4)	4.5
C(15)	0.9047 (5)	0.2068 (6)	0.5360 (4)	4.4
C(16)	0.8996 (4)	0.2326 (5)	0.6070 (4)	3.2
C(21)	0.8596 (4)	0.0536 (5)	0.8533 (4)	3.1
C(22)	0.9121 (4)	0.0261 (6)	0.9191 (4)	3.7
C(23)	0.8730 (5)	−0.0348 (6)	0.9620 (4)	4.6
C(24)	0.7981 (5)	−0.0459 (6)	0.9246 (4)	4.6
C(25)	0.7883 (4)	0.0082 (6)	0.8575 (4)	3.8
C(26)	0.8231 (5)	0.2604 (6)	0.9479 (5)	4.9
C(27)	0.8662 (5)	0.2203 (7)	1.0135 (5)	5.3
C(28)	0.8187 (6)	0.1601 (8)	1.0471 (5)	6.2
C(29)	0.7450 (6)	0.1619 (8)	1.0014 (6)	6.3
C(30)	0.7471 (5)	0.2246 (7)	0.9398 (5)	5.6
C(31)	0.7869 (4)	0.1466 (6)	0.7206 (4)	3.2
C(32)	0.7441 (5)	0.2240 (6)	0.7425 (4)	4.4
C(33)	0.6724 (5)	0.2465 (7)	0.7028 (5)	5.6
C(34)	0.6425 (5)	0.1931 (9)	0.6389 (5)	6.3
C(35)	0.6841 (5)	0.1198 (10)	0.6171 (5)	7.3
C(36)	0.7573 (4)	0.0944 (8)	0.6580 (5)	5.5
C(41)	1.0947 (4)	0.4132 (5)	0.6859 (4)	2.7
C(42)	1.1550 (4)	0.4864 (6)	0.6862 (4)	4.0
C(43)	1.1485 (4)	0.5281 (6)	0.6159 (4)	4.1
C(44)	1.0839 (5)	0.4842 (6)	0.5706 (4)	4.0
C(45)	1.0505 (4)	0.4140 (5)	0.6126 (4)	3.2
C(46)	0.9870 (6)	0.6080 (7)	0.7283 (5)	5.5
C(47)	1.0504 (5)	0.6743 (7)	0.7309 (6)	5.9
C(48)	1.0439 (6)	0.7133 (6)	0.6586 (6)	5.8
C(49)	0.9797 (6)	0.6699 (7)	0.6144 (5)	5.7
C(50)	0.9445 (5)	0.6056 (7)	0.6574 (6)	5.2
C(51)	1.1437 (4)	0.3998 (6)	0.8380 (4)	3.3
C(52)	1.2236 (4)	0.3920 (6)	0.8532 (4)	4.3
C(53)	1.2652 (5)	0.4506 (8)	0.9087 (6)	6.0
C(54)	1.2299 (8)	0.5166 (9)	0.9486 (6)	7.4
C(55)	1.1529 (7)	0.5240 (7)	0.9343 (5)	6.2
C(56)	1.1096 (5)	0.4667 (6)	0.8804 (4)	4.3

of the same phosphine derivative at higher temperature results in a mixture of products that is difficult to characterize.

The structure of **2e**, as determined by X-ray diffraction, is shown in Figure 1. As stated in the introduction, an objective of this work was to trap a ferrocyne fragment; unfortunately, **2e** contains a benzyne moiety. The structure shown was initially proposed for **2e** on the basis of its spectroscopic properties. However, a full structure determination seemed justified because the ^1H NMR spectrum shows some unusual features, especially the chemical shift range of the cyclopentadienyl protons (Figure 3). Also, the microanalytical data are not good in spite of repeated attempts to further purify the compound.

Table III. Selected Bond Lengths (Å) with Esd's in Parentheses

Ru(1)–Ru(2)	2.7748 (8)	Ru(3)–C(12)	2.123 (7)
Ru(1)–Ru(3)	2.7420 (8)	P(1)–C(21)	1.801 (7)
Ru(2)–Ru(3)	2.8983 (8)	P(1)–C(31)	1.829 (7)
Ru(1)–P(1)	2.270 (2)	P(2)–C(41)	1.802 (7)
Ru(1)–C(1)	1.877 (9)	P(2)–C(51)	1.814 (7)
Ru(1)–C(2)	1.867 (9)	C(1)–O(1)	1.133 (10)
Ru(1)–C(7)	2.670 (8)	C(2)–O(2)	1.150 (10)
Ru(1)–C(11)	2.360 (6)	C(3)–O(3)	1.115 (10)
Ru(1)–C(12)	2.318 (6)	C(4)–O(4)	1.155 (10)
Ru(2)–P(1)	2.343 (2)	C(5)–O(5)	1.125 (10)
Ru(2)–P(2)	2.321 (2)	C(6)–O(6)	1.127 (9)
Ru(2)–C(3)	1.970 (9)	C(7)–O(7)	1.122 (10)
Ru(2)–C(4)	1.851 (8)	C(11)–C(12)	1.417 (9)
Ru(2)–C(11)	2.123 (7)	C(11)–C(16)	1.410 (9)
Ru(3)–P(2)	2.380 (2)	C(12)–C(13)	1.438 (10)
Ru(3)–C(5)	1.933 (8)	C(13)–C(14)	1.350 (12)
Ru(3)–C(6)	1.917 (8)	C(14)–C(15)	1.398 (12)
Ru(3)–C(7)	1.957 (9)	C(15)–C(16)	1.379 (11)

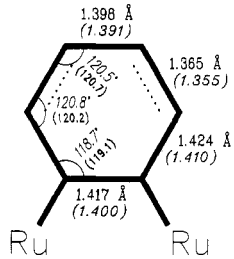

Figure 2. Bond lengths and angles for the benzyne fragment of **2e** and **2b** (in parentheses).

(The NMR studies described below reveal the presence of traces of other compounds in the isolated sample.)

Structure of 2e. The structure of **2e** consists of discrete molecules separated by van der Waals contacts. The cluster consists of a triangle of ruthenium atoms, with two of the edges bridged by phosphido groups; the phosphorus atoms of the bridging groups lie on opposite sides of the Ru_3 triangle. The benzyne ligand is planar ($\chi^2 = 4.895$) and makes an angle of 64.0 (2)° with that of the ruthenium triangle. One side of the benzyne in **2e** spans an edge of the triangle which is bridged by a phosphido group and forms two σ bonds to the ruthenium atoms involved (Ru(2)–C(11) = 2.123 (7) Å; Ru(2)–C(12) = 2.123 (7) Å) and a π bond to the ruthenium atom at the apex of the triangle (Ru(1)–C(11) = 2.360 (6) Å; Ru(1)–C(12) = 2.318 (6) Å). This mode of bonding, $\mu_3\text{-}\eta^2$, has been observed on many occasions in benzyne and acetylene complexes of triangular metal clusters.[4,14–16] The variation of the bond lengths within the benzyne ligand suggest that some degree of bond localization occurs (Figure 2), and the values observed for the bond lengths are in good agreement with those seen in $Ru_3(CO)_7(\mu_3\text{-}C_6H_4)(\mu\text{-}PPh_2)_2$ (**2b**).[3k]

The Ru–C(carbonyl) distances appear to follow a trend seen in previous benzyne clusters; viz., those bonds trans to the σ bonds formed by the benzyne are longer (mean Ru(C) = 1.952 Å) than those which are trans to the π interaction (mean Ru(C) = 1.872 Å), while those to equatorial carbon atoms (C(4), C(6)), which together with a phosphorus atom and one atom of the benzyne occupy a facial site, have intermediate values (mean Ru(C) = 1.885 Å). Carbon atom C(7) which is trans to P(2) has also an

(14) Sappa, F.; Tiripicchio, A.; Braunstein, P. *Chem. Rev.* **1983**, *83*, 203.
(15) Churchill, M. R.; Fettinger, J. G.; Keister, J. B.; See, R. F.; Ziller, J. W. *Organometallics* **1985**, *4*, 2112.
(16) Goudsmit, R. J.; Johnson, B. F. G.; Lewis, J.; Raithby, P. R.; Rosales, M. J. *J. Chem. Soc., Dalton Trans.* **1983**, 2257.

Table IV. Selected Bond Angles (deg) with Esd's in Parentheses

Ru(3)-Ru(1)-Ru(2)	63.38 (2)	P(2)-Ru(2)-P(1)	159.77 (7)	C(41)-P(2)-Ru(2)	127.3 (2)
Ru(1)-Ru(2)-Ru(3)	57.76 (2)	C(11)-Ru(2)-Ru(1)	55.7 (2)	C(41)-P(2)-Ru(3)	116.3 (2)
Ru(2)-Ru(3)-Ru(1)	58.86 (2)	C(11)-Ru(2)-Ru(3)	69.8 (2)	C(51)-P(2)-Ru(1)	119.3 (2)
P(1)-Ru(1)-Ru(2)	54.25 (5)	C(11)-Ru(2)-P(1)	82.2 (2)	C(51)-P(2)-Ru(3)	116.7 (5)
P(1)-Ru(1)-Ru(3)	115.96 (5)	C(11)-Ru(2)-P(2)	83.9 (2)	C(51)-P(2)-C(41)	100.9 (3)
C(11)-Ru(1)-Ru(2)	48.0 (2)	C(11)-Ru(2)-C(3)	167.1 (3)	C(12)-C(11)-Ru(2)	110.1 (5)
C(11)-Ru(1)-Ru(3)	69.9 (2)	C(11)-Ru(2)-C(4)	95.7 (3)	C(16)-C(11)-Ru(2)	131.3 (5)
C(11)-Ru(1)-P(1)	78.9 (2)	P(2)-Ru(3)-Ru(1)	107.31 (5)	C(16)-C(11)-C(12)	118.6 (6)
C(11)-Ru(1)-C(1)	165.4 (3)	P(2)-Ru(3)-Ru(2)	51.03 (5)	C(11)-C(12)-Ru(3)	110.8 (5)
C(11)-Ru(1)-C(2)	102.6 (3)	C(12)-Ru(3)-Ru(1)	55.2 (2)	C(13)-C(12)-Ru(3)	130.4 (5)
C(11)-Ru(1)-C(7)	106.0 (3)	C(12)-Ru(3)-Ru(2)	69.4 (2)	C(13)-C(12)-C(11)	118.8 (5)
C(12)-Ru(1)-Ru(2)	69.6 (2)	C(12)-Ru(3)-P(2)	107.31 (5)	C(12)-C(13)-C(14)	120.5 (7)
C(12)-Ru(1)-Ru(3)	48.7 (2)	C(12)-Ru(3)-C(5)	164.2 (3)	C(13)-C(14)-C(15)	121.0 (7)
C(12)-Ru(1)-P(1)	113.4 (2)	C(12)-Ru(3)-C(6)	95.4 (3)	C(14)-C(15)-C(16)	120.0 (7)
C(12)-Ru(1)-C(1)	147.6 (2)	C(12)-Ru(3)-C(7)	94.3 (3)	C(15)-C(16)-C(11)	121.1 (7)
C(12)-Ru(1)-C(2)	98.5 (3)	Ru(2)-P(1)-Ru(1)	73.93 (5)	C(22)-C(21)-P(1)	126.4 (5)
C(12)-Ru(1)-C(7)	73.3 (2)	C(21)-P(1)-Ru(1)	116.2 (3)	C(25)-C(21)-P(1)	126.3 (6)
C(12)-Ru(1)-C(11)	35.3 (2)	C(21)-P(1)-Ru(2)	125.8 (2)	C(25)-C(21)-C(22)	107.0 (6)
P(1)-Ru(2)-Ru(1)	51.83 (5)	C(31)-P(1)-Ru(1)	121.4 (2)	C(42)-C(41)-P(2)	125.3 (5)
P(1)-Ru(2)-Ru(3)	108.14 (5)	C(31)-P(1)-Ru(2)	117.7 (2)	C(45)-C(41)-P(2)	128.8 (5)
P(2)-Ru(2)-Ru(1)	108.00 (5)	C(31)-P(1)-C(21)	101.8 (3)	C(42)-C(41)-C(42)	105.7 (6)
P(2)-Ru(2)-Ru(3)	52.87 (5)	Ru(3)-P(2)-Ru(2)	76.10 (6)		

intermediate value. All the Ru–C–O angles are linear, 179.2 (7)–176.1 (6)°, save the Ru(3)–C(7)–O(7) angle which is 165.3 (7)°. This carbonyl can be considered to be semibridging as the angle Ru(1)–Ru(3)–C(7) [ψ] is 66.7° which is within the criterion specified by Crabtree and Lavin (ψ < 70°); the Ru(3)–C(7) distance is relatively long (2.670 Å), but it is only some 0.64 Å greater than the sum of the covalent radii and is in the range where significant interaction with Ru(1) would be expected to occur.[17]

The three ruthenium–ruthenium distances within the cluster show a large variation. The longest is that between Ru(2) and Ru(3), 2.898 (1) Å, which is significantly shorter than that seen in the corresponding bond in **2b**, 2.956 (1) Å, and is somewhat longer than that seen in the parent carbonyl [$Ru_3(CO)_{12}$] (average 2.854 Å).[18] It might be thought that if steric effects predominate, the Ru–Ru bonds in **2e** should be longer than in the diphenylphosphino analogue, but this is not the case, suggesting that electronic effects are operative. However, steric effects cannot be totally eliminated as examination of the exocyclic P–C–C angles at C(41) show a marked asymmetry with P(2)–C(41)–C(42), 125.3 (5)°, being less than P(2)–C(41)–C(45), 128.8 (5)°; the cyclopentadienyl ligand is tilted away from the plane of the benzyne ligand to relieve unfavourable steric interactions between H(45) and C(11) (2.681 Å) and C(16) (2.688 Å).

The Ru(1)–Ru(2) bond of intermediate length 2.775 (1) Å in **2e** is in good agreement with the corresponding bond in **2b**, 2.776 (1) Å.[3k] The shortest Ru(1)–Ru(3) bond, 2.742 (1) Å, is spanned by the semibridging CO group and is appreciably shorter than the corresponding bond in **2b** (2.759 (1) Å).

The asymmetric pattern of bonding of the μ-PR_2 groups found in **2a** and **2b** is also present in **2e**.[3,4a] Thus Ru(1)–P(1) = 2.270 (2) Å is shorter than Ru(2)–P(1) = 2.343 (2) Å, lengths which are essentially the same as the corresponding bonds in **2b**. In the other bridging group, Ru(2)–P(2) = 2.321 (2) Å and Ru(3)–P(2) = 2.380 (2) Å are, respectively, the same length and longer than the corresponding bonds in **2b**. This asymmetry has been attributed[3k] to some localization of the M–P(donor) and M–P(phosphido) bonds and/or the presence of a trans interaction with the semibridging CO group only in the case of P(2).

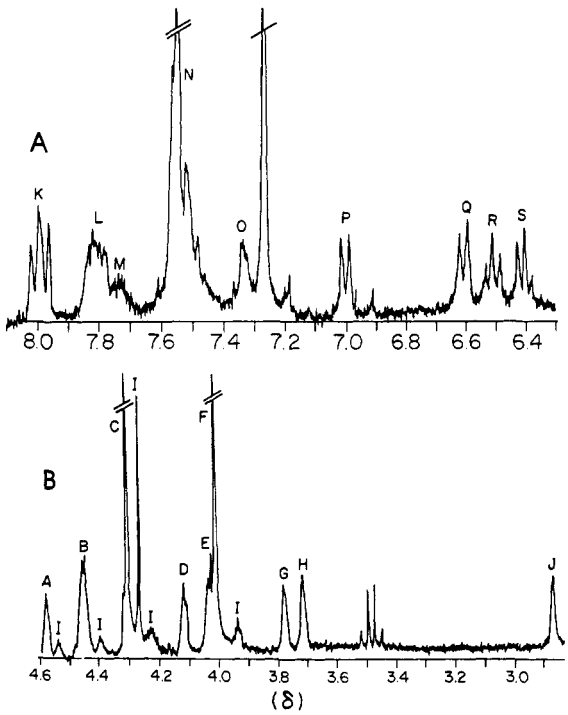

Figure 3. The ^1H NMR spectrum of **2e**: A, the aromatic region; B, the ferrocenyl region.

Spectroscopic Properties of 2e. The pattern of the infrared spectrum of **2e** in the ν(CO) region is similar to that of the osmium derivatives **2a**, **2c**, and **2d**, but there is less resemblance to that of **2b**. The electron-impact mass spectrum is unusually informative;[19] when the probe temperature is 240 °C, it shows a parent peak and stepwise loss of the seven CO groups. At 250 °C the spectrum still shows a parent peak but fewer fragment ions are seen in both the high and low m/e range. The FAB mass spectrum from a tetramethylene sulfone matrix is very similar to the 240 °C electron-impact spectrum.

The ^1H NMR spectrum of **2e** is shown in Figure 3. In the cyclopentadienyl region peaks C and F arise from the two unsubstituted C_5H_5 rings. Peak C is downfield of the usual region observed for ferrocenylphosphines. Decoupling experiments reveal that A, B, G, and H are associated with one monosubstituted cyclopentadienyl group and B,

(17) Crabtree, R. H.; Lavin, M. *Inorg. Chem.* **1986**, *25*, 805.
(18) Churchill, M. R.; Hollander, F. J.; Hutchison, J. P. *Inorg. Chem.* **1977**, *16*, 2655.
(19) Bruce, M. I.; Liddell, M. J. *Appl. Organomet. Chem.* **1987**, *1*, 191.

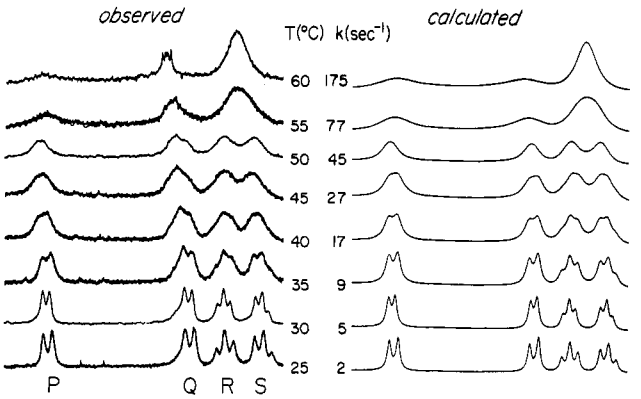

Figure 4. The temperature dependence of the ^1H NMR spectrum of **2e** in the benzyne region.

D, E, and J with the other. This confirms that each ferrocenyl group is monosubstituted. The upfield shift of J is unexpected and indicates some unusual situation for this proton. It is appealing to assign this peak to a proton such as H(45) situated in the vicinity of the benzyne fragment in the solid state (Figure 1). However, the spectrum of **2f**[4a] does not show this feature; the cyclopentadienyl resonances are in the region δ 3.8–4.6 even though the structure is such that the PFcPh unit is situated as in Figure 1 with the Fc group lying above the face of the coordinated benzyne. The peaks labeled I in Figure 3 belong to an impurity which is present in all preparations. The phenyl region of the spectrum of **2e** is also seen in Figure 3. Homonuclear decoupling experiments reveal that K and N, ratio 2:3, are associated with one phenyl group and L, M and O, ratio 2:2:1, with the other.

The presence of the fluxional benzyne fragment, associated with the resonances in Figure 3 labeled PQRS, was first revealed during homonuclear decoupling experiments when irradiation of resonance P resulted in a marked decrease in the intensity of resonance Q. This is an indication that spin saturation transfer is taking place; further results are described in more detail below.

The temperature dependence of the PQRS region of the spectrum is shown in Figure 4. The resonance associated with a small amount of impurity is revealed rather nicely by its different behavior. (This impurity is probably another fluxional benzyne complex.) Also shown in Figure 4 are the simulated spectra and the associated exchange rates.[20] These rates were used to prepare the Eyring plot shown in Figure 5; the data are shown as open circles. The derived parameters are $\Delta H^{\ddagger}$ = 92.8 kJ mol^{-1}, $\Delta S^{\ddagger}$ = 73.2 J K^{-1} mol^{-1}, and thus $\Delta G^{\ddagger}$(278 K) = 72.4 kJ mol^{-1}.[21]

The fluxional process involving the benzyne fragment was further investigated at lower temperatures by using the complementary spin saturation transfer technique first developed by Forsen and Hoffman.[22] The effect of irradiating resonance P on the other benzyne resonances is shown in Figure 6. At 20 °C, irradiating P causes considerable loss of intensity in resonance Q and only some simplification of resonance R. (This was alluded to above.) The same experiment carried out at a series of lower temperatures results in the gradual reappearance of res-

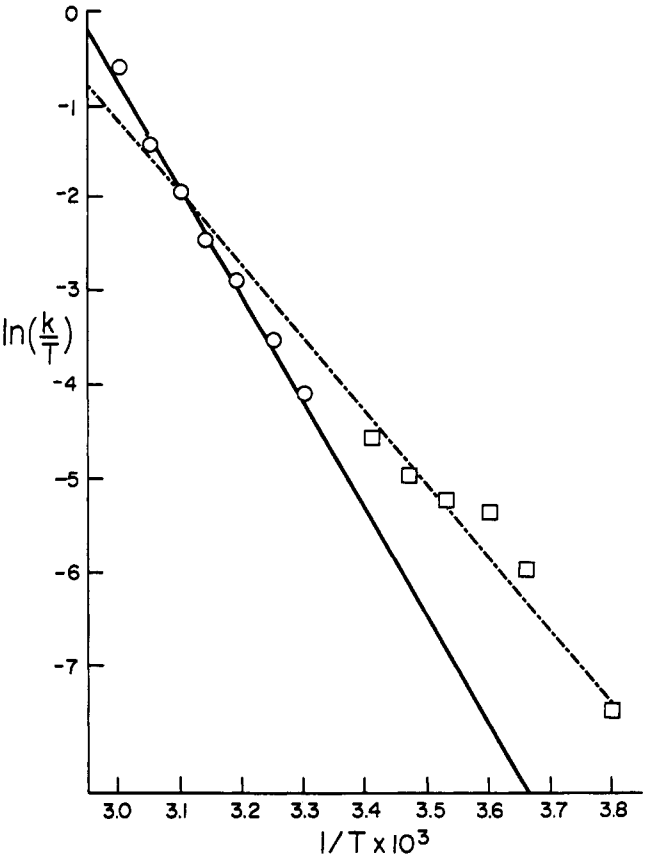

Figure 5. The Eyring plot of the rate data derived from the spectroscopic results shown in Figure 4 (circles) and Figure 6 (squares).

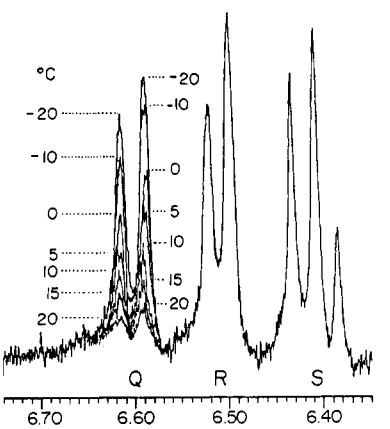

Figure 6. Spin saturation transfer ^1H NMR spectra of the benzyne region of **2e**; resonance P, Figure 3, is being irradiated.

onance Q. The rate constant for this process is given by eq 1, where T_1(Q) = longitudinal relaxation time of nucleus

$$k = \frac{1}{T_1(\mathrm{Q})}\left[\frac{M_0(\mathrm{Q})}{M_z(\mathrm{Q})^{\infty}} - 1\right] \qquad (1)$$

Q, M_0(Q) = magnetization of nucleus Q before perturbation by radio frequency energy, and M_z(Q)$^{\infty}$ = equilibrium magnetization of nucleus Q after perturbation by radio frequency energy.

When the exchanging nuclei are on the same molecule, care should be taken that intramolecular nuclear Overhauser enhancement (NOE) does not interfere with the accuracy of the area measurements. In the present case proton R should be more affected by NOE than proton S, upon irradiation at P, yet both resonances have equal integrals within experimental error. At −20 °C when ex-

(20) Spectroscopic simulation was carried out by using the Program DMR3 General NMR Line-Shape Program with Symmetry and Magnetic Equivalence Factoring by G. Binsch and D. W. Kleier.

(21) Sandström, J. *Dynamic NMR spectroscopy*; Academic: London, 1982.

(22) (a) Forsen, S.; Hoffman, R. A. *Acta Chem. Scand.* **1963**, *17*, 1783. (b) Forsen, S.; Hoffman, R. A. *J. Chem. Phys.* **1964**, *40*, 1189. (c) Forsen, S.; Hoffman, R. A. *J. Chem. Phys.* **1963**, *39*, 2892. (d) Mann, B. E. In *Comprehensive Organometallic Chemistry*; Wilkinson, G., Stone, F. G. A., Abel, E. W., Eds.; Pergamon: Oxford, 1982; Vol. 3, p 89.

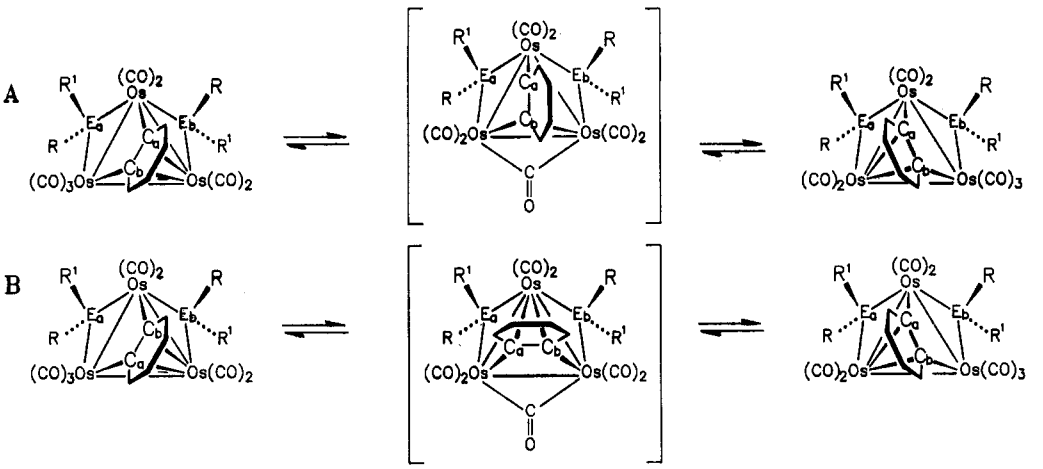

Figure 7. Possible fluxional processes in μ_3-η^2-benzyne derivatives.

Table V. Values of ΔG^* for Benzyne Motion

	4c	4d	2e	2e
T (K)	278[a]	248[a]	278	248
ΔG^* (kJ mol^{-1})	58[b]	51[b]	68.6[c]	67.9[c]

[a] Coalescence temperatures. [b] ΔG^* at coalescence temperature. [c] Calculated value using all data in Figure 5.

change between P and Q is too slow to be observed, the integrals of Q, R, and S are the same within experimental error. Thus NOE does not appear to be a problem. The rate data obtained by this method are also plotted in Figure 5 (as squares). When all the points are included, the dotted line (correlation value 0.987) can be used to obtain data that are different from those mentioned above: $\Delta H^* = 64.0$ kJ mol^{-1} and $\Delta S^* = -16.2$ J K^{-1} mol^{-1}, although $\Delta G^*(278\text{ K}) = 68.6$ kJ mol^{-1} is essentially the same. This situation is not unexpected in view of the error analysis in these procedures described by Sandström.[21]

The benzyne fragment in molecules such as **2a** and **2c** is also fluxional. Deeming and co-workers suggest that at low temperature a fast process interchanges the E_a and E_b bridging groups (Figure 7, path A, e.g. ERR′ = PMe_2) without interchanging the a and b ends of the benzyne fragment.[23] This process also tilts opposite faces of the benzyne fragment toward the plane of the osmium atoms. At higher temperature path B becomes operational and interchange of the a and b ends of the benzyne is achieved. A combination of both pathways results in complete rotation of the benzyne fragment.

In the case of **2e**, the fluxionality detected by the spin saturation transfer experiments exchanges the a and b ends of the benzyne. Thus it cannot be described by path A alone (with E = P, R = Ph, R′ = Fc, and Ru substituted for Os). Path B of Figure 7 interchanges the a and b ends of the benzyne only when R = R′; in this case the two extreme structures are mirror images. When R and R′ are different, as in **2e**, paths A and B need to be combined to obtain the complete rotation necessary to interchange a and b.

The appearance of the plot of Figure 5 seems to suggest that two different fluxional processes are taking place, one which operates above ambient temperature and the other below (Figures 4 and 6). If this view is correct, since both processes would involve interchange of the a and b ends of the benzyne fragment via a 180° rotation, an additional pathway different from that described by the combination of A and B of Figure 7 would be required. This is not inconceivable, but we prefer to believe that we are observing only one fluxional process in **2e**. The similarity of the calculated ΔG^*(278 K) values 68.6 and 72.4 kJ mol^{-1} supports this prejudice. Furthermore spin saturation transfer studies[23] on the complex $H_2Os_3(CO)_9(\mu_3$-η^2-aryne) have established that the motion of the aryne fragment involves C–H (and M–H) bond breaking with concomitant formation of M–H (and C–H) bonds. ΔG^*(363 K) for this process is ~113 kJ mol^{-1} which is much higher than the values listed in Table V. The solid-state structures of **2e** shows that one equatorial carbonyl group is semibridging which may be an indication that a carbonyl exchange process, which would accompany paths A and B, would be favored.

Even if the spin saturation transfer results of Figure 5 are used to calculate ΔG^*, the results are only slightly lower than those quoted in Table V. Thus the motion of the benzyne fragment over the ruthenium cluster is more difficult than over the osmium analogues. This may be due to an increase in steric hindrance in the ruthenium complex because of the presence of the Fc groups; indication of this is seen in the solid-state structure. Otherwise weaker M–C bonds and a greater tendency to form bridging carbonyls could be expected to result in easier motion in the ruthenium complex relative to the osmium one. Clearly more studies are needed.

Acknowledgment. We thank the Natural Sciences and Engineering Research Council of Canada for financial assistance, Johnson Matthey Limited for the loan of ruthenium salts, and Dr. B. E. Mann for very helpful discussions.

Registry No. **2e**, 116324-27-7; $Ru_3(CO)_{10}(PFcPh_2)_2$, 116324-26-6.

Supplementary Material Available: Tables of hydrogen atom positions (Table VI) and anisotropic thermal parameters (Tables VII) (5 pages); a table of calculated and observed structure factors (Table VIII) (25 pages). Ordering information is given on any current masthead page.

(23) ΔG^* for path A of Figure 7, ERR′ = PMe_2, is estimated to be ~31 kJ mol^{-1}.[3d]

(24) Kneuper, H.-J.; Shapley, J. R. *Organometallics* **1987**, *6*, 2455.